

# USE OF VERTICAL-RADAR PROFILING TO ESTIMATE POROSITY AT TWO NEW ENGLAND SITES AND COMPARISON WITH NEUTRON LOG POROSITY

*Marc L. Buursink, CGISS, Boise State University, Boise, ID*

*John W. Lane Jr., OGW-BG, U.S. Geological Survey, Storrs, CT*

*William P. Clement, CGISS, Boise State University, Boise, ID*

*Michael D. Knoll, CGISS, Boise State University, Boise, ID*

## Abstract

Vertical-radar profiles (VRPs) and neutron porosity logs were acquired at two sites in New England – Haddam Meadows State Park in Connecticut and Massachusetts Military Reservation on Cape Cod. Both sites include boreholes drilled to depths from 30 to 50 meters into unconsolidated fluvial or glacial sediments. The VRP data are inverted using Tikhanov regularization to obtain interval radar propagation velocities. Of the two sites, the radar velocities at Haddam Meadows State Park show more variability with depth because this site consists of poorly sorted fluvial sediments, whereas the radar velocities at Cape Cod show much less variability because this site consists of well-sorted glacial sediments.

The interval radar propagation velocities from the VRPs are converted to estimates of saturated sediment porosity using the Topp and time-propagation petrophysical models. VRP-derived porosities are compared to neutron log-derived porosities and yielded a correlation between values derived from the two methods. Lack of correlation between the VRP-derived porosities and the neutron log-derived porosities at some depths may be explained by discrepancy in the sample volume of each method, by problems in the petrophysical models, or by differences in borehole construction methods used at each site. Overall correlation between the VRP-derived porosities and the neutron log-derived porosities supports the advantage of deriving porosities from VRP data due to the decreased cost and ease of data acquisition, and simple processing and inversion routines.

## Introduction

Vertical-radar profiling (VRP) provides a detailed profile of radar propagation velocity with depth in a borehole. VRP data acquisition and analysis is similar to vertical seismic profiling (VSP). VSP has been used for many years in the petroleum industry, primarily to calibrate surface seismic reflection data (Hardage, 1985). VSP also has been used for obtaining interval seismic velocities using travel-time inversion (Stewart, 1984). Until recently, the cost of borehole radar instrumentation has made common use of VRP prohibitive, but commercial manufacturers have now introduced lower-cost borehole radar systems. As a result, VRP has been used for different applications, including archeology (Zhou and Sato, 2000) and physical property estimation (Knoll and Clement, 1999).

VRPs are collected by recording the direct radar-wave arrivals with the borehole-radar transmitting antenna located on the surface and the receiving antenna located in the borehole. The travel-times of the direct arrivals are inverted to give interval radar propagation velocity as a function of depth. Based on the radar propagation velocity, the dielectric permittivity variation with depth is then calculated. Using a couple of simple petrophysical relations given below, porosity values are derived from the dielectric permittivity values.

In this paper, the VRP method is demonstrated using data collected at two sites in New England - Haddam Meadows State Park (HMSP) in Connecticut and Massachusetts Military Reservation (MMR) on Cape Cod. The lithologies of the two sites show different amounts of grain-size heterogeneity. To assess the reliability of the material property estimates, the VRP-derived porosities are compared to porosity values determined from neutron logging. The results suggest that the VRP method can provide accurate, high-resolution porosity estimates at borehole locations.

## Vertical-Radar Profiling Data Collection

VRP data were collected in July 2001, in one borehole each at HMSP and at MMR. HMSP is located in south-central Connecticut, along the Connecticut River. Based on drilling tailings, the lithology at HMSP consists of river-deposited unconsolidated, poorly sorted, interbedded coarse, medium and fine sands with very little silt or clay (House and others, 1995). Data were collected in borehole JL-3. MMR is located on Cape Cod where the Cape meets the mainland. Based on lithologic logging, the lithology at MMR consists of well-sorted homogeneous unconsolidated medium to coarse sands (LeBlanc, 1984). Data were collected in borehole FSW-626E.

In the field, VRP data are acquired using a Malå Geoscience<sup>1</sup> RAMAC/GPR system with 100 MHz borehole antennas. The radar system uses fiber optic cables to connect the antennas with the control unit and, thus, eliminate cross talk and standing electromagnetic (EM) waves in the borehole. The transmitting antenna is placed on the ground surface and oriented radially to the borehole axis to minimize polarization mismatch with the receiving antenna. The transmitting antenna is not moved during the course of the VRP survey. The center (feedpoint) of this antenna was 1.01 meters (m) from the borehole axis. The receiving antenna is located downhole to insulate it from sources of cultural EM noise. Depths below measurement point are referenced to the feedpoint of the receiving antenna. The receiving antenna is lowered manually but continuously by a single operator down the borehole with a trace collected every five centimeters (**Figure 1**). An optical depth encoder tracks the antenna depth and triggers the control unit. Each trace is stacked 64 times to improve the signal to noise ratio.

---

<sup>1</sup> The use of firm, trade, and brand names in this paper is for identification purposes only and does not constitute endorsement by the U.S. Geological Survey.

## Vertical-Radar Profiling Data Processing

The VRP data are the amplitude (voltage) of the EM energy as a function of time for each receiver depth (or source-receiver offset). Our goal is to determine the arrival-time of the energy that propagates directly through the subsurface from the transmitter to the receiver. As the radar system is an imperfect recording device there are systematic errors in the amplitude and timing of direct arrivals. The data are processed to reduce these errors.

To ensure accurate radar propagation velocity estimates, compensated sampling frequency and time-zero corrections are applied to the data. The corrections account for sampling mismatch and lag time of the radar system electronics. Using a surface walk-away acquisition geometry and the known speed of light, the compensated sampling frequency is calculated by adjusting the slope of the airwave arrival time versus antenna offset relation. The compensated sampling frequency converts the sample number of the direct arrival pick to the true arrival time. Then, the time-zero correction for actual pulse onset is calculated by timing the airwave arrival at different offsets and extrapolating the time of this arrival to a zero offset.

In addition to the corrections above, the following processing steps are applied: the trace headers are edited to insure correct transmitter and receiver antenna positions and associated offset, the direct-current bias is removed on a trace-by-trace basis to facilitate wiggle trace plotting, and the automatic gain control is applied to improve the display of the first arrivals. The direct-current bias is a systematic error in recorded amplitude values that results in the data not having a zero mean voltage.

To select the travel-times of the direct arrivals, the first peak of the energy onset is picked. First peaks are picked rather than first breaks because first peaks are identified more confidently. Error in picking occurs when the phase of the signal onset waveform changes or when the signal to noise ratio increases. Because of signal to noise limits, the HMSP data were picked down to 22 m, and the MMR data were picked down to 27 m.

## Inversion for Radar Interval Velocities

Following direct arrival picking and travel time corrections, the travel time and antenna position data are inverted to obtain interval velocity values with depth down the borehole (**Figures 2 and 3**). The velocity inversion process consists of two steps - forward modeling and then inversion. The forward model in the first step computes the ray paths between the transmitter and the receiver positions. To linearize the inverse problem, the ray paths are approximated with straight rays, a valid assumption for long rays traveling below the water table, and each layer is assigned a constant velocity and thickness. Instead of arbitrarily choosing the layer thickness, we use Akaike information criterion (AIC) to find the optimal number of layers (Clement, in review). AIC includes the number of model parameters (layers) to determine the goodness of fit. Including the number of model layers balances the trade-off between improving the data fit with more parameters and over-fitting the data and its noise. As a result of the optimization, the subsurface is modeled as 0.5-m thick horizontal layers. In the second step

weighted-damped least-squares with Tikhonov regularization is used to invert the data. The routine uses the pseudo-inverse, based on singular-value decomposition, to find the inverse of the over-determined system of equations. The regularization trade-off is adjusted until the residual error normalized by the degrees of freedom (data minus parameters) approaches one or slightly greater than one.

## Estimation of Porosity

Previous researchers have used surface and borehole ground-penetrating radar (GPR) data to estimate hydraulic properties (Greaves and others, 1996; Hubbard and others, 1997). In this paper, the inverted interval velocities ( $v$ ) are used to calculate dielectric permittivities ( $K$ ), using equation 2, the speed of light constant ( $c$ ), and assuming low loss (Greaves and others, 1996).

$$K = \left( \frac{c}{v} \right)^2 \quad (1)$$

Next, two simple petrophysical models are used to convert the dielectric permittivity values ( $K$ ) to porosity ( $\theta$ ) values – the Topp equation (2) (Topp and others, 1980) and the time propagation (TP) relation (3) (Wharton and others, 1980; Knoll and Knight, 1994).

$$\theta = -5.3 \cdot 10^{-2} + 2.92 \cdot 10^{-2}(K) - 5.5 \cdot 10^{-4}(K^2) + 4.3 \cdot 10^{-6}(K^3) \quad (2)$$

$$\theta = \frac{\sqrt{K} - \sqrt{K_{matrix}}}{\sqrt{K_{water}} - \sqrt{K_{matrix}}} \quad (3)$$

Because TP is a mixing model, the saturated subsurface at the two study sites is modeled as a two-phase system, which is assumed to consist of fresh water and sand matrix components. No other components, such as clays or metallic minerals are considered. To ensure a good fit, the fresh water dielectric permittivity ( $K_{water}$ ) is assumed to be 81, whereas the sand matrix dielectric permittivity ( $K_{matrix}$ ) is assumed to be 8. The Topp equation is an empirical relation, and does not account for subsurface lithology or minerology.

The VRP-derived porosities for both sites are compared to porosities estimated from neutron logs collected at both sites. The neutron logs also were collected in July 2001. Full saturation is assumed, so only data below the water table are plotted. A conventional neutron porosity probe records the rate at which neutrons from a source on the probe are scattered back to one or more detectors (Hearst and others, 2000). The measured backscatter count rate is inversely proportional to the total water content in the region surrounding the probe. A dual-detector neutron probe designed to reduce sensitivity to the presence of water in the borehole and calibrated at the American Petroleum Institute neutron calibration pit (Hodges, 1988) was used for this study. The neutron log data were collected in 0.1-foot intervals, but were smoothed with an eleven-point moving average to yield about a 1 foot volume of investigation.

For the MMR borehole, the combined plots of VRP-derived and neutron-log porosity values show only small variations with depth (**Figure 4**). The means of both the VRP-derived and neutron-log porosity values are similar. No general trend of increasing or decreasing porosity down the borehole is observed. The maximum and minimum porosity values for both the VRP-derived and neutron-log are similar but do not correlate with depth. Porosity trends for

both the VRP-derived and neutron-log values do correlate over several intervals. For example, the trend in porosity on the neutron-log from 11 to 13 m below measurement point (BMP) also is seen in the Topp and TP porosity estimates. Other correlated trends in porosity occur from 15 to 17 m, and from 18 to 21 m BMP. Porosity values for the VRP-derived and neutron-log do not correlate over several other intervals, including those from 9 to 11 m BMP, from 21 to 22 m BMP, and from 24 to 25 m BMP. In these cases the porosity trends are of opposite magnitudes.

For the HMSP borehole, the combined plots for the VRP-derived and neutron-log porosity values show more variation with depth (**Figure 5**). Nevertheless, the means of both the VRP-derived and neutron-log porosity values are similar. A general trend of increasing porosity with borehole depth down to 13 m BMP is observed. The minimum porosity values for both the VRP-derived and neutron-log are similar but do not correlate with depth. A couple of zones of anomalously high values for VRP-derived porosity exist. Porosity trends for both the VRP-derived and neutron-log correlate over several intervals, including from 5 to 6 m BMP, from 7 to 10 m BMP, from 13 to 15 m BMP, and from 16.5 to 17.5 m BMP. Porosity trends for both the VRP-derived and neutron-log do not correlate over several other intervals, including those from 10 to 13 m BMP, from 15 to 16.5 m BMP, and from 19 to 20 m BMP. At both sites, the Topp-derived porosities tend to be about 10 percent higher than the TP-derived porosities because each model is derived based on a different set of empirical data and mixing laws.

## Concluding Discussion

Overall, a correlation is present between the VRP-derived and neutron-log porosity estimates for boreholes at the HMSP and MMR sites. Porosity differences between VRP-derived and neutron-log values can be explained by the discrepancy between the sample volumes of the two methods and by the limitations in the models used to convert dielectric permittivity to porosity. In typical sediments with typical saturated porosity values (5-50%), the neutron log sample volume is about 0.8 m in diameter (Hearst and others, 2000). In contrast, the VRP sample volume is integrated from the land surface down in 0.5 m layers. The VRP measures properties more strongly on one half of the borehole, whereas the neutron log averages data from around the borehole.

Limitations in the petrophysical models, such as an oversimplified lithology or mineralogy model of the subsurface, may cause an incorrect conversion from dielectric permittivity to porosity. Differences between the model-derived porosities and the neutron-log porosities may be explained by variations in the dielectric permittivity of the matrix material that were modeled incorrectly rather than by the change in the magnitude of porosity with depth. Nevertheless, the effect of variable mineralogy on the measured dielectric permittivity of sediments is only second-order and is therefore not very significant.

To better address the issue of correlation of VRP-derived porosities and neutron-log porosities, a controlled test is needed. As part of the controlled test, porosity values can be independently measured over a range of different volume scales.

Because of more rigorous drilling practices used at the MMR borehole, less anomalous values are observed in the VRP-derived and neutron-log results. The borehole was drilled by minimizing the size of the auger-disturbed zone and by filling the borehole annulus with native sand collapse material against the screen and casing. The borehole construction at HMSP was not as rigorous as at MMR, and therefore the borehole annulus may have been washed out during drilling or not back-filled with native collapse material. This problem may be responsible for the anomalously high VRP-derived porosities.

Due to decreased disturbance of the annular space during borehole drilling at MMR, the porosity data correlated better at this site than at HMSP. Another explanation for the discrepancy in porosity value variation with depth is that the material at HMSP has a very heterogeneous grain-size distribution, whereas the material at MMR has a fairly homogeneous grain-size distribution (House and others, 1995; LeBlanc, 1984). In a previous study at the Boise Hydrogeophysical Research Site, the VRP-derived and neutron-log porosity data correlated well following a smooth trend with depth (Knoll and Clement, 1999). The smaller-scale porosity variations observed in the neutron logging did not correlate with the VRP-derived data. At this site the more rigorous drilling practices were also applied.

The advantages of deriving porosities from VRP data include the decreased cost and ease of data acquisition, and simple processing and inversion routines. Sources of error in using the VRP data include inaccurate picks of first arrivals and non-uniqueness between material porosity and material dielectric permittivity estimates. Neutron-log porosities more directly measure the material porosity but are expensive, have an added risk because of the radioactive source, and are sensitive to variations in borehole construction.

## Acknowledgments

The authors gratefully acknowledge Fred Paillet, Richard Hodges, and Barbara Corland of the USGS for acquisition and processing of the neutron-log data. We thank the U.S. Air Force Center for Environmental Excellence at the Massachusetts Military Reservation, Cape Cod, Massachusetts, and the State of Connecticut Department of Environmental Protection for permission to access boreholes. We thank Peter Joesten and Michael Lambert of the USGS for assistance with geophysical logging. We thank Fred Paillet of the USGS and Warren Barrash of CGISS at BSU for their colleague reviews of the paper. Contribution number 0119 of the Center for Geophysical Investigation of the Shallow Subsurface at Boise State University.

## References

1. Clement, W. P., "Choosing the optimal model dimension based on Akaike's information and related criteria", *Geophysics*, in review.
2. Greaves, R.J., D.P. Lesmes, J.M. Lee, and M.N. Toksoz (1996), "Velocity variations and water content estimated from multi-offset, ground-penetrating radar", *Geophysics*, v. 61, no. 3, p. 683-695.

3. Hardage, B.A. (1985), *Vertical Seismic Profiling: Part A: Principles*, 2nd ed. London: Geophysical Press, 552 p.
4. Hearst, J.R., P.H. Nelson, and F.L. Paillet (2000), *Well logging for physical properties: A Handbook for Geophysicists, Geologists, and Engineers*, 2nd ed., New York, Wiley, 483 p.
5. Hodges, R.E. (1988), "Calibration and standardization of geophysical well-logging equipment for hydrologic applications", *Water-Resources Investigations Report*, 88-4058, U. S. Geological Survey, 25 p.
6. House, J.R., T.M. Boyd, and F.P. Haeni (1995), "Haddam Meadows, CT--A case study for the acquisition, processing, and relevance of the 3-D seismic reflection method as applied to near-surface concerns", in *Expanded Abstracts with Author's Biographies*, SEG International Exposition and 65th Annual Meeting, Houston, Texas, October 8-13, 1995: Tulsa, Oklahoma, Society of Exploration Geophysicists, p. 411-414.
7. Hubbard, S.S., J.E. Peterson Jr., E.L. Majer, P.T. Zawislanski, K.H. Williams, J. Roberts, and F. Wobber (1997), "Estimation of permeable pathways and water content using tomographic radar data", *Leading Edge--Near-Surface Geophysics*, Knight, Rosemary, ed., v. 16, no. 11, p. 1623-1628.
8. Knoll, M.D. and W.P. Clement (1999), "Vertical radar profiling to determine dielectric constant, water content and porosity values at well locations", in *Symposium on the Application of Geophysics to Engineering and Environmental Problems Proceedings*, Oakland, CA: Environmental and Engineering Geophysical Society, Wheat Ridge, CO, p. 821-830.
9. Knoll, M.D. and R. Knight (1994), "Relationships between dielectric and hydrogeologic properties of sand-clay mixtures", *Fifth International Conference on GPR Proceedings*, 12-16 June 1994, Kitchener, Ontario, p. 45-61.
10. LeBlanc, D.R. (1984), "Sewage plume in a sand and gravel aquifer, Cape Cod, Massachusetts", *Water-Supply Paper*, 2218, U. S. Geological Survey, Reston, VA. 28 p.
11. Stewart, R.R. (1984), "VSP interval velocities from travelttime inversion", *Geophysical Prospecting*, v. 32, p. 608-628.
12. Topp, G.C., J.L. Davis, and A.P. Annan (1980), "Electromagnetic determination of soil water content; measurements in coaxial transmission lines", *Water Resources Research*, v. 16, no. 3, p. 574-582.

13. Wharton, R.P., G.A. Hazen, R.N. Rau, and D.L. Best (1980), “Electromagnetic propagation logging”, *Advances in Technique and Interpretation*, Presented at the 55th Annual Technical Conference, Society of Petroleum Engineers of AIME, Paper SPE 9267, 12 p.
14. Zhou, H. and M. Sato (2000), “Application of vertical radar profiling technique to Sendai Castle”, *Geophysics*, v. 65, no. 2, p. 533-539.



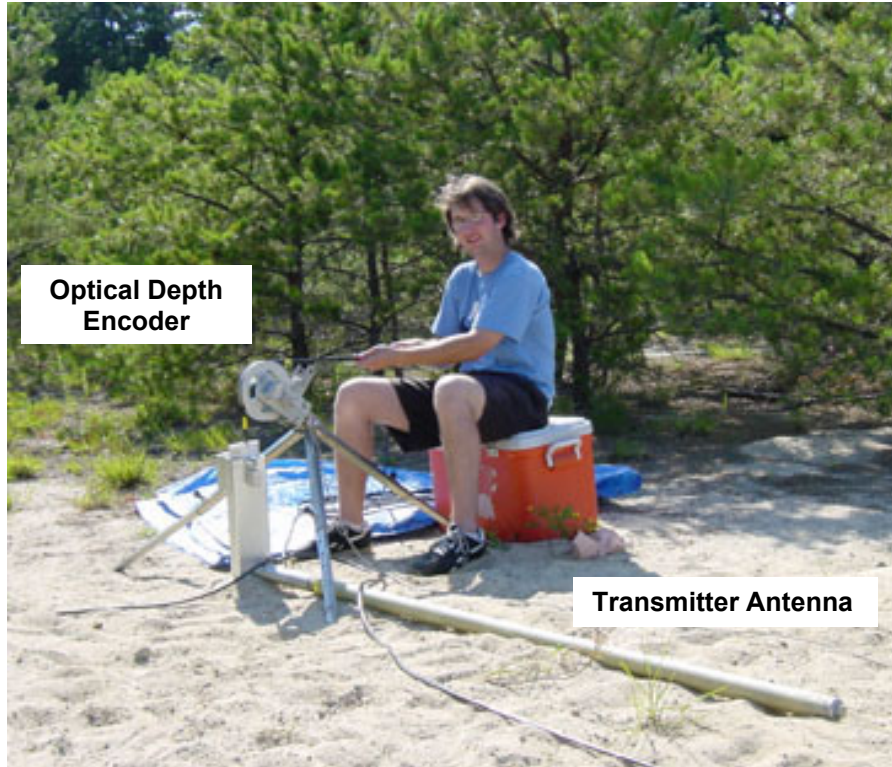


**Figure 1. Vertical radar profiling data acquisition in the field. The transmitter antenna is located on the surface radially outward from the borehole. The receiver antenna is manually and continuously lowered down the borehole so that a trace is collected every 0.05 meter, triggered by an optical depth encoder.**

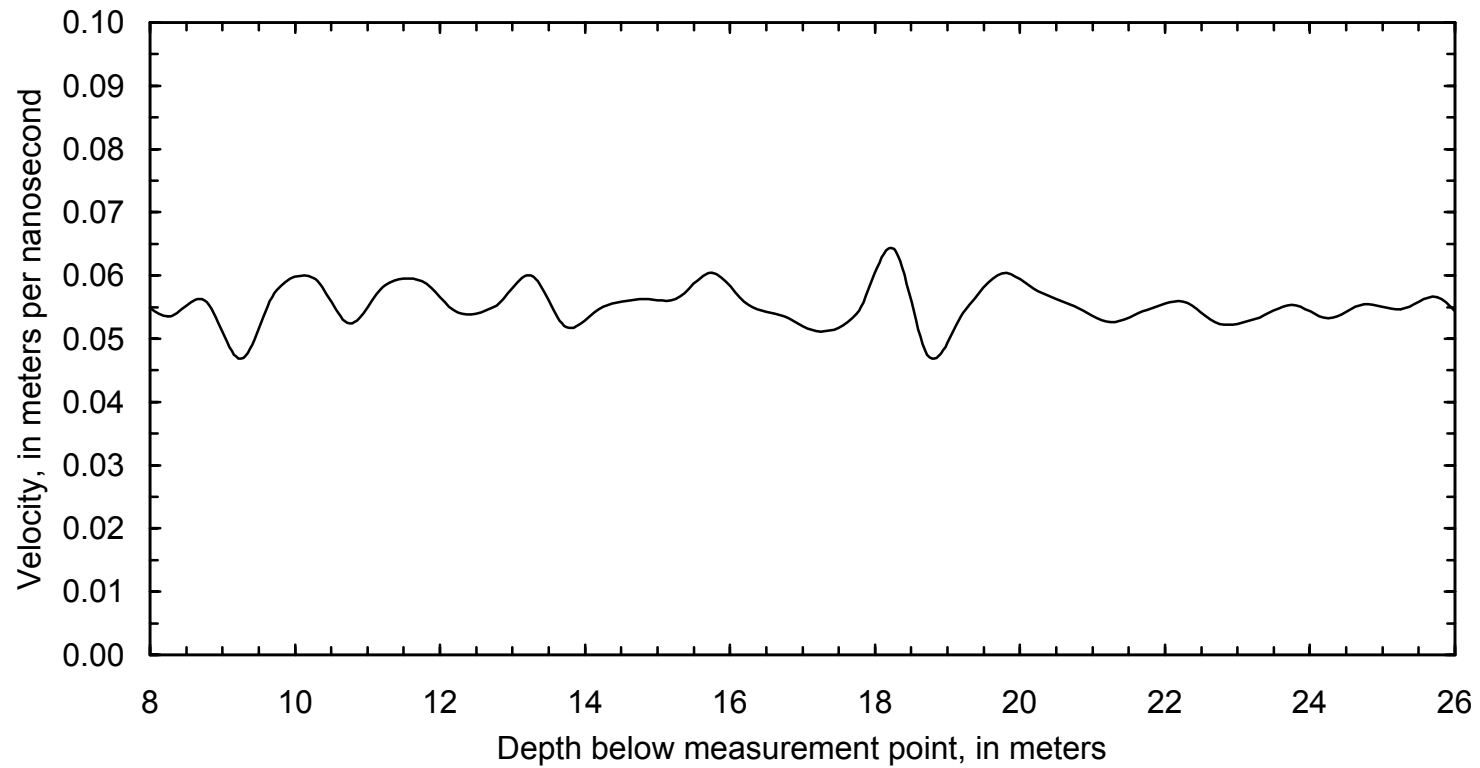


**Figure 2. Vertical radar profile-derived radar propagation velocities for borehole FSW-626E at the Massachusetts Military Reservation, Cape Cod.**

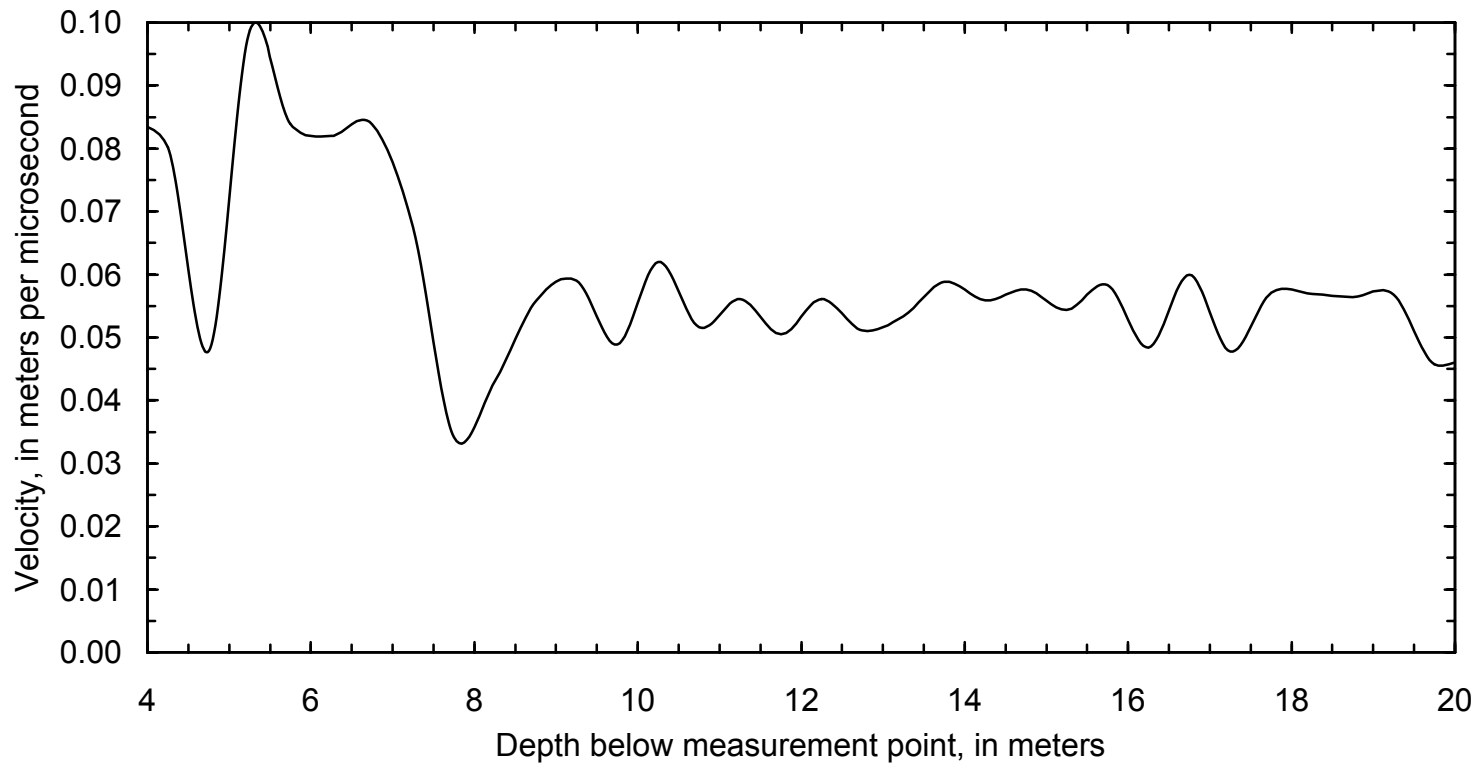


**Figure 3. Vertical radar profile-derived radar propagation velocities for borehole JL-3 at Haddam Meadows State Park, Connecticut.**

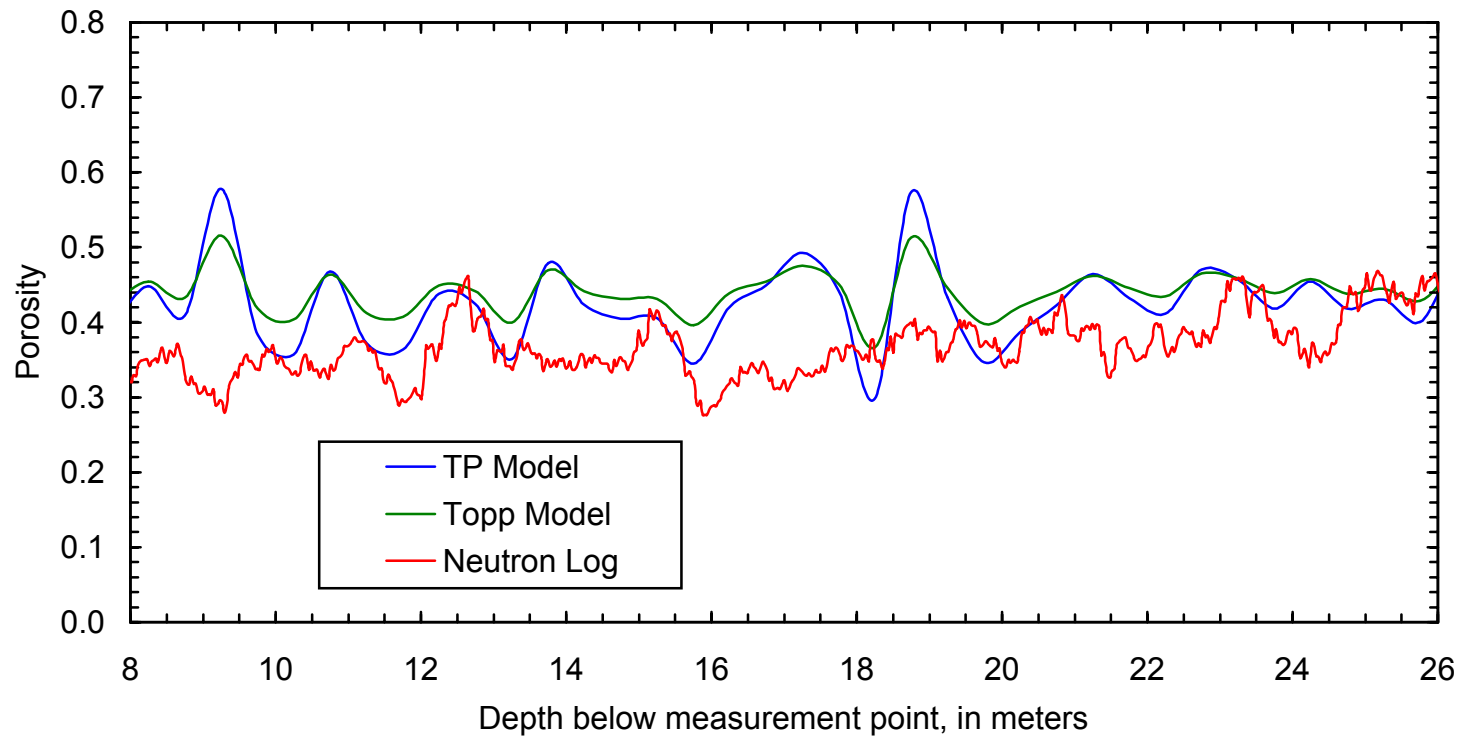


**Figure 4. Vertical radar profile-derived porosities using Topp and TP models compared to neutron log porosities for borehole FSW-626E at the Massachusetts Military Reservation, Cape Cod.**

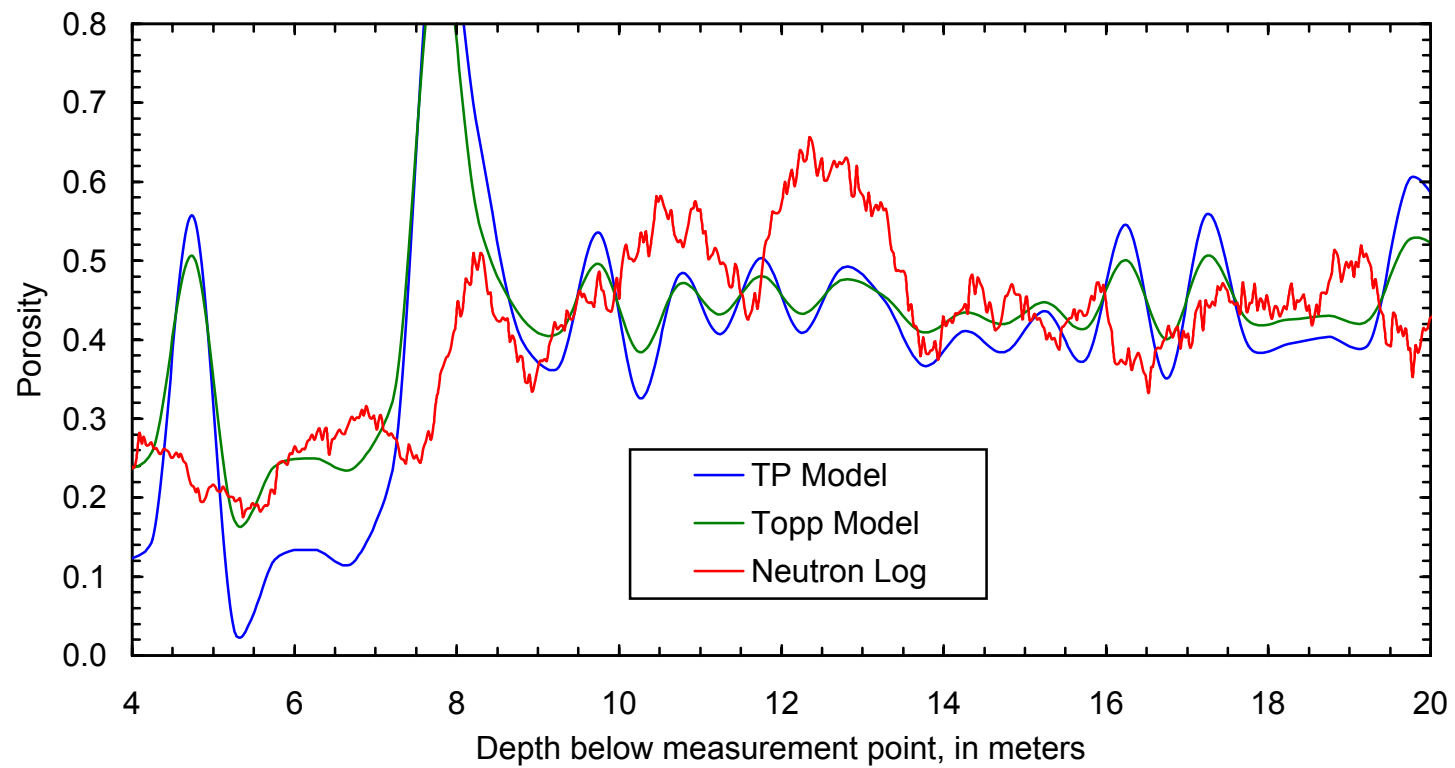


**Figure 5. Vertical radar profile-derived porosities using Topp and TP models compared to neutron log porosities for borehole JL-3 at Haddam Meadows State Park, Connecticut.**